Desalination and Water Treatment
www.deswater.com
doi: 10.1080/19443994.2013.815687

52 (2014) 6104–6112
September

Taylor & Francis
Taylor & Francis Group

Adsorptive removal of methylene blue using the natural adsorbent-banana leaves

R.R. Krishni[a], K.Y. Foo[b], B.H. Hameed[a,*]

[a]*School of Chemical Engineering, Engineering Campus, Universiti Sains Malaysia, Nibong Tebal, Penang 14300, Malaysia*
Tel. +604 5996422; Fax: +604 5941013; email: chbassim@eng.usm.my
[b]*Environment and Occupational Health Programme, School of Health Sciences, Health Campus, Universiti Sains Malaysia, Kubang Kerian, Kelantan 16150, Malaysia*

Received 16 June 2012; Accepted 23 May 2013

ABSTRACT

In this work, the banana leaf, an agricultural waste, widely used for wrapping of food was utilized as a low-cost adsorbent for removing methylene blue (MB) dye from the aqueous solution. The effects of initial concentration, contact time, and solution pH on the adsorption performance were investigated in a batch mode study at 30°C. The adsorptive uptake of MB increased with increasing the initial MB concentration and solution pH. Equilibrium data were simulated using the Langmuir and Freundlich isotherms, pseudo-first-order, pseudo-second-order and intraparticle diffusion models. The data were well fitted to the Langmuir isotherm model, showing a maximum monolayer adsorption capacity of 109.89 mg/g. Adsorption kinetics were best described by the pseudo-second-order and intraparticle diffusion models. The results illustrated the potential use of waste banana leaves for the removal of colors and dyes from the textile wastewater.

Keywords: Adsorption; Banana leaves; Equilibrium; Isotherm; Kinetic; Methylene blue

1. Introduction

Over the past several decades, the percolation of textile effluents into the waterways and aquifer systems has remained a fastidious concern among the environmentalists [1]. In particular, textile industries consume large volumes of water and chemicals for wet processing of textiles. These textile wastewaters are usually a mixture of large complexes, particulates, processing assistants, salts, surfactants, acids and alkalis, which diverse widely in chemical composition, ranging from inorganic compounds to polymers and organic products [2]. Numerous studies have been conducted to assess the harmful impacts of colorants on the ecosystem. The real hazard setting aside esthetic considerations is exacerbated when the colored agents interfere with the transmission of light through water, retard photosynthetic activities in aquatic life, inhibit the growth of biota, and damage the quality of the receiving streams, thus upsetting biological processes within streams, resulting in an ecological imbalance [3].

A developing research by the invention of a broad array of treatment technologies (precipitation, coagulation–flocculation, sedimentation, flotation, filtration,

*Corresponding author.

1944-3994/1944-3986 © 2013 Balaban Desalination Publications. All rights reserved.

membrane processes, electrochemical techniques, biological process, chemical reactions, adsorption, and ion exchange) has stimulated a dramatic progress in the scientific community [4–13]. Of major interest, activated carbon adsorption process, an adsorbent with its large porous surface area, controllable pore structure, thermo-stability and low acid/base reactivity, is recognized as the most efficient and promising fundamental approach in wastewater treatment [14]. Despite its prolific use in adsorption processes, the biggest barrier of the application by the industries is the cost-prohibitive adsorbent and difficulties associated with regeneration [15]. Realizing the complications, a growing exploration to evaluate the reliability of natural, renewable and low cost materials as alternative adsorbents in water or air pollution control has been exerted [16].

In the perspective, banana (*Musa sapientum*), the leading edible member of the family Musaceae found abundantly in tropical and subtropical area, is a herbaceous plant with a height of 2–8 m, and leaves of 3.5 m in length [17]. Banana is cultivated primarily for its fruit, and it bears fruit only once throughout its lifetime. According to the Department of Agricultural online database, the annual production of banana in Malaysia was 270,000 T in 2010, corresponding to a biomass residue yield of 649,000 T [18]. In the common practice, banana leaves are used as plates for lining cooking pits and for wrapping of food. However, this will eventually turn into waste after it has served its purposes. Researches were carried out intended to recycle the used banana leaves and convert these wastes into a profitable end commodity, which formulate the motivation of this study. The focus of this study was to evaluate the adsorptive potential of waste banana leaves for removing methylene blue (MB) dye from aqueous solutions. Textural and functional characterization of the prepared adsorbent was performed. Moreover, the effects of initial dye concentration, contact time, pH, isotherms, kinetics and mechanisms on the adsorptive uptake of MB were outlined.

2. Materials and methods

2.1. Adsorbate

MB, C.I. Classification Number 52,015, chemical formula = $C_{16}H_{18}N_3ClS$, MW = 319.85, λ_{max} = 668 nm (purity = ⩾ 82%), supplied by Sigma-Aldrich (M) Sdn. Bhd, Malaysia was chosen as the adsorbate in this study and was not purified prior to used. Deionized water supplied by USF ELGA water treatment system was used to prepare all the reagents and solutions.

2.2. Preparation and characterization of adsorbent

Used banana leaves required in this study were obtained locally. The precursor was firstly washed to remove dirt particles from its surface, cut into small pieces (1–3 cm) and dried in an oven at 70 °C. The dried sample was then ground and sieved to discrete sizes (200–300 μm), washed repeatedly with hot distilled water, dried overnight at 70 °C, and stored in plastic containers. Scanning electron microscopy (SEM) analysis was performed to study the textural structure of adsorbent before and after the adsorption of dyes. Surface functional groups of the prepared adsorbent were detected by Fourier transform infrared (FTIR) spectroscope (FTIR-2000, PerkinElmer) in the scanning range of 4,000–400 cm^{-1}.

2.3. Batch equilibrium studies

The batch equilibrium studies were conducted in a set of 250-mL Erlenmeyer flasks containing 0.30 g of adsorbent and 200 mL of MB solutions with the initial concentrations of 50–300 mg/L without adjusting pH. The flasks were capped and agitated in an isothermal water bath shaker at 120 rpm and 30 °C until the equilibrium was reached. Sample solutions were withdrawn at equilibrium to determine the residual concentrations. All samples were filtered (Whatman 0.45 μm) prior to analysis to minimize the interference of adsorbent fines with the analysis. The concentrations of MB in the supernatant solutions before and after the adsorption process were analyzed using a double-beam UV–vis spectrophotometer (Shimadzu UV-1601, Japan) at its maximum wavelength of 668 nm. Each experiment was duplicated under identical conditions. The MB uptake at equilibrium, q_e (mg/g), was calculated by:

$$q_e = \frac{(C_0 - C_e)V}{W} \quad (1)$$

where C_0 and C_e (mg/L) are the liquid-phase concentrations of dye at initial and equilibrium, respectively. V is the volume of the solution (L), and W is the mass of adsorbent used (g).

2.4. Effect of solution pH

The effect of solution pH on the adsorptive uptake of MB was examined by varying the initial pH from pH 2 to 10, at the fixed MB concentration of 200 mg/L, adsorbent dosage of 0.15 g/100 mL and adsorption temperature of 30 °C. The pH was adjusted using 0.1 M HCl or NaOH solution and measured using a pH meter (Model Ecoscan, EUTECH Instruments, Singapore).

2.5. Batch kinetic studies

The procedure of adsorption kinetic study was identical to the batch equilibrium studies, where the aqueous samples were withdrawn at different time intervals and the concentrations of MB were similarly measured. The amount of adsorption at time t, q_t (mg/g), was calculated by:

$$q_t = \frac{(C_0 - C_t)V}{W} \quad (2)$$

where C_t (mg/L) is the liquid-phase concentrations of dye at time t (min).

3. Results and discussion

3.1. Characterization of the prepared adsorbent

Fig. 1 illustrates SEM images of the banana leave derived adsorbent before and after the sorption of MB. It can be clearly found that the adsorbent surface exhibited a heterogeneous and high pores structure. However, the surface of the dye-loaded adsorbent displayed a rougher texture, covered with the adsorbed dye molecules.

The obtained FTIR spectrum (Table 1) revealed the peaks at 3,410, 3,123, 1,621, 1,517, 1,431–1,320, 1,376, 1,242–1,159, 1,060, 897, 783, and 665 cm^{-1}, corresponded to the presence of –OH (hydroxyl), C=C (alkynes), $–NH_2$,$–NH_3^+$, C–O–H, $–CH_3$, C–O–C (esters, ether or phenol), P–H, Si–H, out-of-plane C–H, and C–O–H functional groups. Meanwhile, the surface chemistry of the banana leave derived adsorbent detected some shift, disappear and new peaks after the sorption of MB, indicating possible involvement of the functional groups during the adsorption process

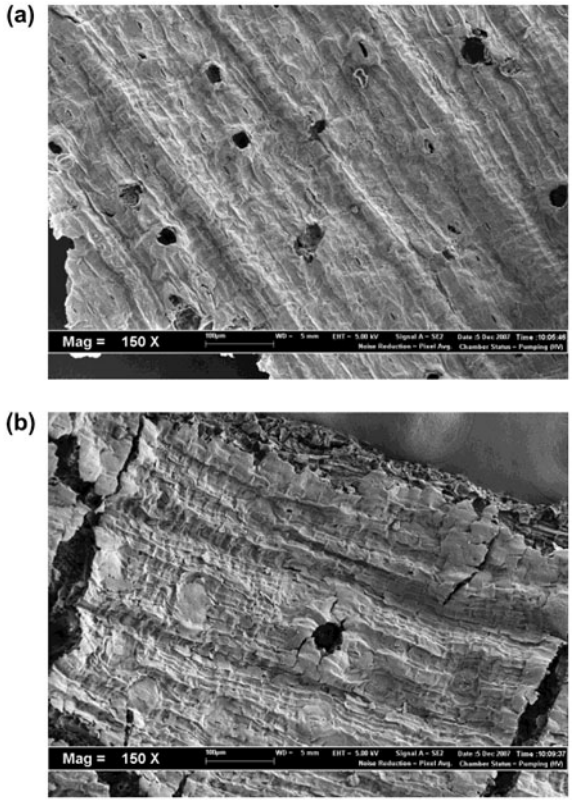

Fig. 1. SEM micrograph (150 X) for the banana leaves adsorbent (a) before and (b) after the adsorption of MB.

3.2. Effects of initial concentration and contact time on the adsorption equilibrium

Fig. 2 shows the effects of contact time and initial dye concentration on the adsorption of MB at 30°C. Generally, the adsorptive uptake of MB increased with prolonging the contact time. Initially, the amount of MB adsorbed onto the adsorbent surface increased rapidly, and at some point of time, the process slowed down and reached a plateau. At this point, the amount of dye desorbing from the adsorbent is in a state of dynamic equilibrium with the amount of dye being adsorbed onto the adsorbent. The time required to attain this state of equilibrium is termed as equilibrium time, and the amount of dye adsorbed at the equilibrium reflected the maximum adsorption capacity of the adsorbent under those operating conditions. This phenomenon was attributed to the fact that a large number of vacant surface sites were available during the initial stage, and after a lapse of time, the remaining vacant surface sites were difficult to be occupied due to repulsive forces between the solute molecules on the solid and bulk phases. Similar trend was observed in the adsorption of MB onto gypsum and natural zeolite [19,20].

Initial concentration provides an important driving force for alleviating mass transfer resistances of dye molecules between aqueous solution and the solid phases. Hence, in the present study, the adsorption equilibrium of MB, q_e increased from 31.67 to 101.32 mg/g with an increase in initial concentration from 50 to 300 mg/L. This process takes relatively longer contact time and the time profile of dye uptake is a single, smooth and continuous curve leading to saturation, suggesting possible monolayer coverage of dye onto the surface of adsorbent [21]. At lower concentrations of 50–100 mg/L, the ratio of initial number of dye molecules to the available surface area is low, subsequently, the fractional adsorption become

Table 1
Comparison of FTIR Spectroscopy of the banana leaves derived adsorbent before and after the adsorption of MB

Frequency (cm^{-1})			
IR peak	Before adsorption	After adsorption	Assignment
1	3,410	3,395	Bonded –OH groups
2	2,123	–	C=C stretch
3	1,621	1,602	NH_2 deformation
4	1,517	1,490	NH_3^+ deformation
5	1,431	1,438	C–O–H stretch
6	1,320	1,334	C–O–H stretch
7	1,376	1,391	CH_3 deformation
8	1,242	1,246	C–O–C stretch
9	1,159	–	C–O–C stretch
10	1,060	1,100	P–H deformation
11	–	1,038	S=O stretch
12	897	885	Si–H deformation
13	–	809	CH out-of-plane deformation
14	783	785	CH out-of-plane deformation
15	–	706	NH deformation
16	665	667	C–O–H twist broad
17	–	627–500	C–H stretch

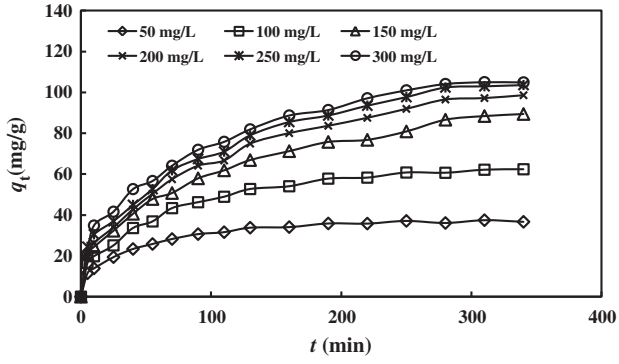

Fig. 2. Effects of initial concentration and contact time on the adsorption of MB onto banana leaves derived adsorbent (conditions: $W = 0.30$ g/200 mL; temperature = 30 °C).

independent on the initial concentration. However, at higher concentration of 150–300 mg/L, the availability of adsorption sites become fewer (saturation of the sorption sites) and longer contact time of 280 min were required for MB solutions to reach to the equilibrium. Royer et al. [22] reported that the equilibrium time for the adsorption of MB onto Brazilian pine-fruit shell was 5–10 h for an initial concentration of 300 and 500 mg/L, while Ahmad et al. [23] has discovered that for an initial concentration of 200 mg/L, the amount of MB adsorbed onto meranti sawdust was rapidly high at the beginning of adsorption, and the saturation level was gradually reached within 4 h. This illustrates that the adsorption performance of the prepared adsorbent was comparable with the works carried out by previous researchers.

3.3. Effect of solution pH on dye adsorption

Fig. 3 depicts the effect of solution pH on the adsorptive uptake of MB. Increasing solution pH from 2 to 10 indicated an increasing q_e from 22.37 to 109.90 mg/g. The maximum q_e was observed at pH 7 where no significant changes were noticed beyond the value. This behavior is due to the protonation of MB in the acidic medium, and development of positive charge onto the adsorbent surface, inhibiting the accessibility of the pores structure [24]. Moreover, it is associated with the presence of excess H^+ ions, which present a competitive impact with dye molecules for the adsorption sites. However, in the basic medium, the formation of electric double layer changes its polarity and consequently the dye uptake increases. The result is in good agreements with the previous findings [25,26].

3.4. Adsorption isotherm

Adsorption isotherms are viable for describing the relationship between adsorbate molecules and the adsorbent surface and highlight the distribution of adsorbate molecules between the liquid and solid phases [27]. In this study, two common isotherm models were established: the Langmuir and Freundlich isotherm models. The applicability of the isotherm equation was judged by the determination of correlation coefficients, R^2.

Langmuir isotherm [28] assumes monolayer adsorption, with adsorption can only occur at a finite number of localized sites that are identical and energetically equivalent. The mathematical expression of Langmuir isotherm is defined as follows:

$$q_e = \frac{Q_0 K_L C_e}{1 + K_L C_e} \tag{3}$$

where Q_0 (mg/g) and K_L (L/g) are Langmuir constants related to adsorption capacity and energy of adsorption. The linear form of Langmuir isotherm is defined as:

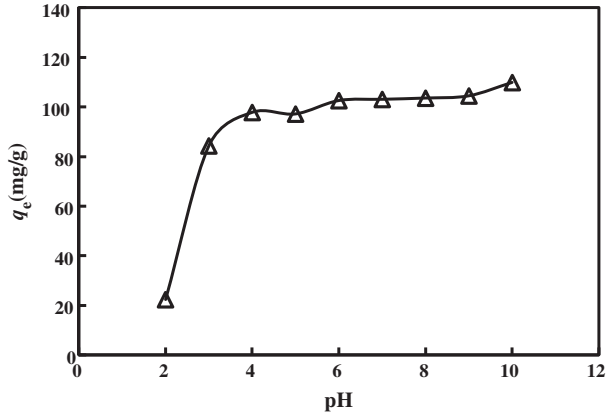

Fig. 3. Effect of solution pH on the adsorption of MB onto banana leaves derived adsorbent (conditions: $W = 0.30\,g/200\,mL$; $C_0 = 250\,mg/L$; temperature 30°C).

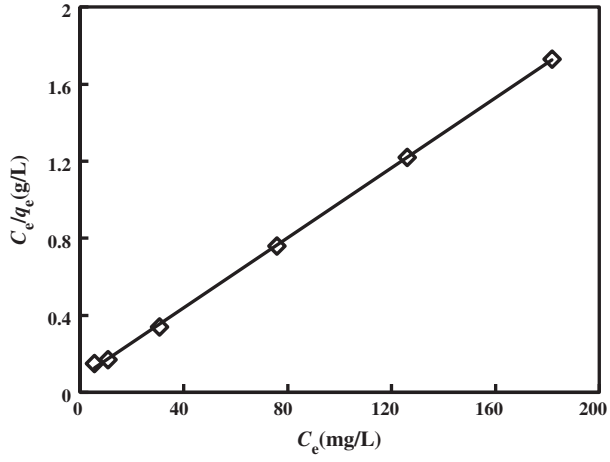

Fig. 4. Plot of Langmuir isotherm for the adsorption of MB onto banana leaves derived adsorbent at 30°C.

$$\frac{C_e}{q_e} = \frac{1}{Q_0 K_L} + \frac{1}{Q_0} C_e \quad (4)$$

When C_e/q_e is plotted against C_e, a straight line with the slope $1/Q_0$ and the intercept $1/Q_0$ K_L can be obtained.

Fig. 4 and Table 2 show the linear plot of Langmuir isotherm model couple with its isotherm constants. The equilibrium data were getting valid for Langmuir isotherm model, with the R^2 higher than 0.99 at 30°C. The applicability of Langmuir isotherm model suggested that the adsorption process is monolayer with each molecule poses equal enthalpies and activation energy. The results also demonstrated that there is no interaction and transmigration of dyes in the plane of the neighboring surface.

Freundlich isotherm model [29] is an empirical equation describing the nonideal and reversible adsorption. The model can be applied to multilayer adsorption, with nonuniform distribution of adsorption heat and affinities over the heterogeneous surface. The model is expressed as follows:

$$q_e = K_F C_e^{\frac{1}{n}} \quad (5)$$

where K_F (mg/g (l/mg)$^{1/n}$) and n are Freundlich constants related to adsorption capacity and adsorption intensity of the adsorbent. K_F can be defined as adsorption coefficient and represents the quantity of dye adsorbed onto adsorbent for a unit of equilibrium concentration. The magnitude of the exponent, $1/n$ below one represents normal Langmuir isotherm while $1/n$ above one is indicative of cooperative adsorption. The linear form of Freundlich isotherm is as follows:

$$\log q_e = \log K_F + \frac{1}{n} \log C_e \quad (6)$$

Fig. 5 displays the linear plot of the Freundlich isotherm model, and Table 2 lists the isotherm constants determined from the intercept and slope. The correlation coefficient, R^2 fitted with Freundlich isotherm model (0.860) was found much lower than the Langmuir isotherm model (0.999), thus ascertained the monolayer coverage of MB onto the prepared adsorbent. Table 3 exhibits a comparison of monolayer adsorption capacities of MB onto various adsorbents [30–38]. The adsorbent prepared in this work showed relatively high adsorption capacity for MB of 109.89 mg/g, as compared to some previous works as reported in the literature.

Table 2
Langmuir and Freundlich isotherm parameters for the adsorption of MB onto banana leaves derived adsorbent

Langmuir isotherm model				Freundlich isotherm model		
Q_o (mg/g)	b (L/mg)	R^2	Separation factor, R_L	K_F (mg/g) (L/mg)$^{1/n}$	n	R^2
109.89	0.116	0.9996	0.03	26.92	3.33	0.8602

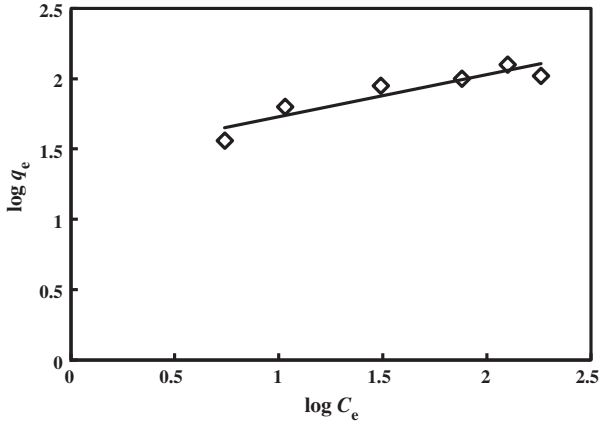

Fig. 5. Plot of Freundlich isotherm for the adsorption of MB onto banana leaves derived adsorbent at 30°C.

3.5. Adsorption kinetics

Adsorption kinetics describe the solute uptake, which in turn govern residence time of the adsorption process [39]. When adsorption is preceded by diffusion through a boundary, the kinetics in most systems follow the pseudo-first-order kinetic equation. Lagergren [40] proposed pseudo-first-order kinetic model in the form of:

$$\log\left(\frac{q_e}{q_e - q_t}\right) = \frac{k_1}{2.303}t \tag{7}$$

where k_1 is the adsorption rate constant (1/min). The value of k_1 was obtained from the slopes of the linear plots of log $[q_e/(q_e-q_t)]$ vs. t, as shown in Fig. 6(a). The corresponding results are tabulated in Table 4. The R^2 values, which ranged between 0.976 and 0.897, were relatively small. Moreover, the experimental q_e values did not agree satisfactory with the calculated q_e values obtained theoretically. This showed that the adsorption of MB onto the banana leaves based adsorbent did not follow pseudo-first-order equation.

Contrary to the other models, pseudo-second-order kinetic equation [41] predicts the behavior over the whole range of adsorption, with chemisorption being the rate controlling step. The pseudo-second-order kinetic model is expressed as:

$$\frac{t}{q_t} = \frac{1}{k_2 q_e^2} + \frac{1}{q_e}t \tag{8}$$

where k_2 (g/mg min) is the pseudo-second-order kinetic rate constant. The linear plot of t/q_t versus t gave $1/q_e$ as the slope and $1/k_2\, q_e^2$ as the intercept. The linear plot of t/q_t versus t, as shown in Fig. 6(b)

Table 3
Comparison of monolayer adsorption capacities of various adsorbents for MB

Adsorbent	Q_0 (mg/g)	T (°C)	Reference
Used banana leaves	109.89	30	Present study
Tea waste	85.16	27	[30]
Pathenium (PWC)	20.80	30	[31]
Wheat shells	16.56	30	[32]
Yellow passion fruit peel	0.0068	25	[33]
Wheat straw	3.82	30	[34]
Waste apricot-based activated carbon	102.04	30	[35]
Rice husk	40.58	32	[36]
Orange peel	18.60	30	[37]
Bamboo dust activated carbon	143.20	30	[38]

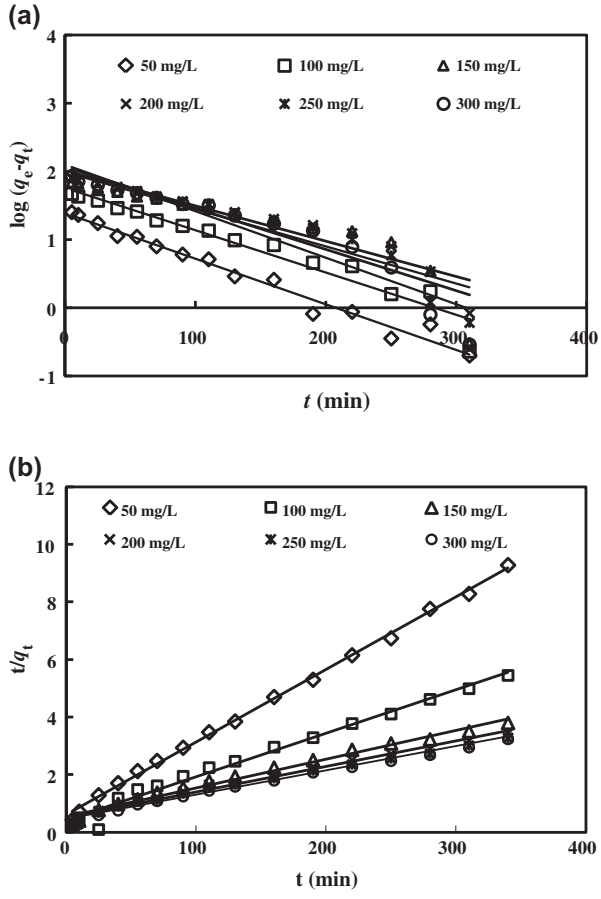

Fig. 6. Plots of (a) pseudo-first-order and (b) pseudo-second-order kinetic models for the adsorption of MB onto banana leaves derived adsorbent at 30°C.

Table 4
Kinetic models parameters for the adsorption of MB onto banana leaves derived adsorbent at different initial MB concentrations

C_o (mg/L)	$q_{e,\ exp}$ (mg/g)	Pseudo-first-order kinetic model			Pseudo-second-order kinetic model		
		$q_{e1,\ cal}$ (mg/g)	k_1 (1/min) 10^{-1}	R^2	$q_{e2,\ cal}$ (mg/g)	k_2 (g/mg min) 10^{-3}	R^2
50	36.64	24.48	0.15	0.9764	39.68	1.05	0.9979
100	62.36	57.44	0.14	0.9369	66.23	0.56	0.9826
150	90.05	97.41	0.13	0.8052	100.00	0.19	0.9825
200	99.85	103.30	0.12	0.9063	112.36	0.16	0.9839
250	103.06	115.82	0.14	0.9060	119.05	0.15	0.9823
300	104089	124.62	0.16	0.8969	119.05	0.18	0.9886

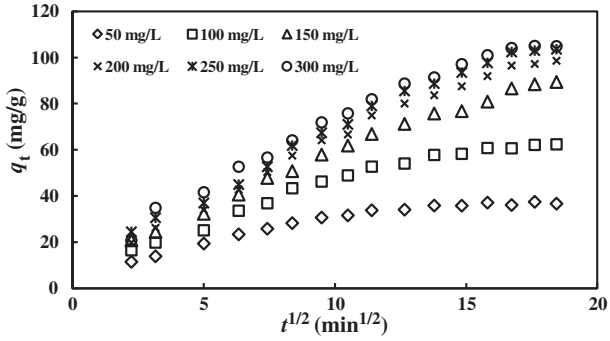

Fig. 7. Plots of Intraparticle diffusion model for different initial MB dye concentrations at 30°C.

revealed good agreement with the pseudo-second-order kinetic model, with the correlation coefficients greater than 0.98 for all MB concentrations. Additionally, the calculated q_e did not differ notably with the experimental q_e (Table 4). This suggested that the adsorption process was controlled by chemisorption, which involved valency forces through electrons sharing between MB and the adsorbent.

To examine the adsorption mechanism of the adsorption system, the Weber and Morris intraparticle diffusion model [42] was applied to analyze the equilibrium data. According to the theory, the Weber and Morris intraparticle diffusion model is derived as follows:

$$q_t = k_{id} t^{1/2} + C \tag{9}$$

where C is the intercept and k_{id} is the intraparticle diffusion rate constant (mg/g min$^{0.5}$). If pore diffusion is the rate-limiting step, then the plot q_t versus $t^{0.5}$ gives a straight line with the slope, k_{pi} and the intercept, C_i; and intraparticle diffusion is the sole rate limiting step if the plot passes through the origin. The values of intercept, C, give an idea about the thickness of boundary layer, where the larger the intercept, the greater is the boundary layer effect.

The intraparticle diffusion plots for the adsorption of MB onto the banana leaves derived adsorbent for the concentration of 50–300 mg/L was presented in Fig. 7. The values of k_{id}, C_i and correlation coefficients, R^2 obtained for the plots are given in Table 5. The first, sharper region is the instantaneous adsorption or external surface adsorption, representing the mass transfer of adsorbate molecules from the bulk solution to the adsorbent surface. The second region is the gradual adsorption stage where intraparticle diffusion is rate limiting. The third region, exists in some cases,

Table 5
Intraparticle diffusion model parameters for the adsorption of MB onto banana leaves derived adsorbent for different initial MB concentrations at 30°C

C_o (mg/L)	$K_{id,\ 1}$ (mg/h$^{1/2}$g)	C	R_1^2	$K_{id,\ 2}$ (mg/g min$^{1/2}$)	C	R_2^2
50	2.70	5.62	0.9968	0.70	25.02	0.8576
100	4.08	6.88	0.9908	1.44	36.80	0.9457
150	5.14	8.27	0.9967	3.34	28.81	0.9809
200	5.90	6.46	0.9955	3.43	37.01	0.9734
250	5.97	9.72	0.9923	3.43	42.45	0.9587
300	6.23	11.99	0.9891	3.11	50.94	0.9355

is the final equilibrium stage where intraparticle diffusion started to slow down due to the extremely low adsorbate concentrations left in the solutions [43].

As can be seen from Fig. 7, the linear lines of the second stages did not pass through the origin, due to the difference in the mass transfer rate in the initial and final stages of adsorption. The deviation also exhibited the presence of multilinearity, indicating the transportation of adsorbate from solution phase to the surface of adsorbent is controlled by a combination of more than one step (film or external diffusion, pore diffusion, surface diffusion and adsorption onto the pore surface) [44]. This implied that intraparticle diffusion was not the only rate-limiting mechanism in the adsorption process. Increasing bulk liquid dye concentrations from 50 to 300 mg/L showed an enhancement of pore diffusion rate and intercept, indicative of the increase of thickness of the boundary layer and driving force for the sorption process.

4. Conclusion

The present investigation revealed the versatility of banana leaves developed adsorbent for removing MB dye from aqueous solutions over a wide range of concentrations. Adsorption data were best described by the Langmuir isotherm model, with a monolayer adsorption capacity of 109.89 mg/g. The kinetic data agreed satisfactory with the pseudo-second-order kinetic model, suggesting a chemisorption process.

References

[1] A. Ojstrsek, D. Fakin, Colour and TOC reduction using biofilter packed with natural zeolite for the treatment of textile wastewaters, Desalin. Water Treat. 33 (2011) 147–155.

[2] E. Ellouze, D. Ellouze, A. Jrad, R.B. Amar, Treatment of synthetic textile wastewater by combined chemical coagulation/membrane processes, Desalin. Water Treat. 33 (2011) 118–124.

[3] K.Y. Foo, B.H. Hameed, An overview of dye removal via activated carbon adsorption process, Desalin. Water Treat. 19 (2010) 255–274.

[4] J.Y.K. Li, B.L. Zhao, L.J. Zhang, R.P. Han, Biosorption of copper ion by natural and modified wheat straw in fixed-bed column, Desalin. Water Treat. (2013), doi: 10.1080/19443994.2012.762945.

[5] R. Schurer, A. Janssen, L.O. Villacort, M. Kennedy, Performance of ultrafiltration and coagulation in an UF-RO seawater desalination demonstration plant, Desalin. Water Treat. 42 (2012) 57–64.

[6] J. Nan, W.P. He, Characteristic analysis on morphological evolution of suspended particles in water during dynamic flocculation process, Desalin. Water Treat. 41 (2012) 35–44.

[7] M. Sivanatham, B.V.R. Tata, C.A. Babu, Synthesis of crown ether functionalized polyacrylamide gel beads and their extraction behaviour for strontium ions, Desalin. Water Treat. 38 (2012) 8–14.

[8] D.S. Filho, G.B. Bota, R.B. Borri, F.J.C. Teran, Eletrocoagulation/flotation followed by fluidized bed anaerobic reactor applied to tannery effluent treatment, Desalin. Water Treat. 38 (2012) 8–14.

[9] K.Y. Foo, B.H. Hameed, Decontamination of textile wastewater via TiO_2/activated carbon composite materials, Adv. Colloid Interface Sci. 159 (2010) 130–143.

[10] A. Lerch, N. Siebdrath, P. Berg, V. Gitis, W. Uhl, Fouling minimised reclamation of secondary effluents with reverse osmosis (ReSeRO), Desalin. Water Treat. 42 (2012) 181–188.

[11] K.Y. Foo, B.H. Hameed, A short review of activated carbon assisted electrosorption process: An overview, current stage and future prospect, J. Hazard. Mater. 170 (2009) 552–559.

[12] H.Q. Chu, Y.L. Zhang, B.Z. Dong, X.F. Zhou, D.W. Cao, Z.M. Qiang, Z.X. Yu, H.W. Wang, Pretreatment of micro-polluted surface water with a biologically enhanced PAC–diatomite dynamic membrane reactor to produce drinking water, Desalin. Water Treat. 40 (2012) 84–91.

[13] K.Y. Foo, B.H. Hameed, The environmental applications of activated carbon/zeolite composite materials, Adv. Colloid Interface Sci. 162 (2011) 22–28.

[14] K.Y. Foo, B.H. Hameed, Potential of activated carbon adsorption processes for the remediation of nuclear effluents: A recent literature, Desalin. Water Treat. 41 (2012) 72–78.

[15] K.Y. Foo, B.H. Hameed, Recent developments in the preparation and regeneration of activated carbons by microwaves, Adv. Colloid Interface Sci. 149 (2009) 19–27.

[16] Md. Ahmaruzzaman, Adsorption of phenolic compounds on low-cost adsorbents: A review, Adv. Colloid Interface Sci. 143 (2008) 48–67.

[17] H.P.S.A. Khalil, M.S. Alwani, A.K.M. Omar, Chemical composition, anatomy, lignin distribution and cell wall structure of Malaysian plant waste fibers, BioResources 17 (2006) 220–232.

[18] Department of Agriculture, Malaysia, 2012. Available online at: http://www.doa.gov.my/statistik/buah03-08.htm. (accessed April 2012).

[19] M.A. Rauf, S.M. Qadri, S. Ashraf, K.M. Al-Mansoori, Adsorption studies of Toluidine Blue from aqueous solutions onto gypsum, Chem. Eng. J. 150 (2009) 90–95.

[20] R. Han, J. Zhang, P. Han, Y. Wang, Z. Zhao, M. Tang, Study of equilibrium, kinetic and thermodynamic parameters about methylene blue adsorption onto natural zeolite, Chem. Eng. J. 145 (2009) 496–504.

[21] M. Hema, S. Arivoli, Comparative study on the adsorption kinetics and thermodynamics of dyes onto acid activated low cost carbon, Int. J. Phys. Sci. 2 (2007) 10–17.

[22] B. Royer, N.F. Cardoso, E.C. Lima, J.C.P. Vaghetti, N.M. Simon, T. Calvete, R.C. Veses, Applications of Brazilian pine-fruit shell in natural and carbonized forms as adsorbents to removal of methylene blue from aqueous solutions-kinetic and equilibrium study, J. Hazard. Mater. 164 (2009) 1213–1222.

[23] A. Ahmad, M. Rafatullah, O. Sulaiman, M.H. Ibrahim, R. Hashim, Scavenging behaviour of meranti sawdust in the removal of methylene blue from aqueous solution, J. Hazard. Mater. 170 (2009) 357–365.

[24] J.Q. Liang, J.H. Wu, P. Li, X.D. Wang, B. Yang, Shaddock peel as a novel low-cost adsorbent for removal of methylene blue from dye wastewater, Desalin. Water Treat. 39 (2012) 70–75.

[25] Q. Zhou, W.Q. Gong, C.X. Xie, Y.B. Li, C.P. Bai, S.H. Chen, Biosorption of methylene blue from aqueous solution on spent cottonseed hull substrate for *Pleurotus ostreatus* cultivation, Desalin. Water Treat. 29 (2011) 317–325.

[26] E.I. Unuabonah, G.U. Adie, L.O. Onah, O.G. Adeyemi, Multistage optimization of the adsorption of methylene blue dye onto defatted Carica papaya seeds, Chem. Eng. J. 155 (2009) 567–579.

[27] K.Y. Foo, B.H. Hameed, Insights into the modeling of adsorption isotherm systems, Chem. Eng. J. 156 (2010) 2–10.

[28] I. Langmuir, The adsorption of gases on plane surfaces of glass, mica and platinum, J. Am. Chem. 57 (1918) 1361–1403.

[29] H. Freundlich, Über die adsorption in lösungen (Adsorption in solution), Z. Phys. Chem. 57 (1906) 384–470.

[30] M.T. Uddin, M.A. Islam, S. Mahmud, M. Rukanuzzaman, Adsorptive removal of methylene blue by tea waste, J. Hazard. Mater. 164 (2009) 53–60.
[31] H. Lata, V.K. Grag, R.K. Gupta, Removal of a basic dye from aqueous solution by adsorption using *Parthenium hysterophorus*: an agricultural waste, Dyes Pigm. 74 (2007) 653–658.
[32] Y. Bulut, H. Aydin, A kinetics and thermodynamics study of methylene blue adsorption on wheat shells, Desalination 194 (2006) 259–267.
[33] F.A. Pavan, A.C. Mazzocato, Y. Gushiken, Removal of methylene blue dye from aqueous solutions by adsorption using yellow passion fruit peel as adsorbent, Bioresour. Technol. 99 (2008) 3162–3165.
[34] F. Batzias, D. Sidiras, E. Schroeder, C. Weber, Simulation of dye adsorption on hydrolyzed wheat straw in batch and fixed-bed systems, Chem. Eng. J. 148 (2009) 459–472.
[35] C.A. Basar, Applicability of the various adsorption models of three dyes adsorption onto activated carbon prepared waste apricot, J. Hazard. Mater. 135 (2006) 232–241.
[36] V. Vadivelan, K.V. Kumar, Equilibrium, kinetics, mechanism, and process design for the sorption of methylene blue onto rice husk, J. Colloid Interface Sci. 286 (2005) 90–100.
[37] G. Annadurai, R.S. Juang, D.J. Lee, Use of cellulose-based wastes for adsorption of dyes from aqueous solutions, J. Hazard. Mater. 92 (2002) 263–274.
[38] N. Kannan, M.M. Sundaram, Kinetics and Mechanism of removal of methylene blue by adsorption on various carbon-comparative study, Dyes Pigm. 51 (2001) 25–40.
[39] X.H. Xue, X.S. He, Y.H. Zhao, Adsorptive properties of acid-heat activated rectorite for Rhodamine B removal, equilibrium, kinetics studies, Desalin. Water Treat. 37 (2012) 259–267.
[40] S. Langergren, About the theory of so-called adsorption of soluble substances, Kungliga Svenska Vetenskapsakademies Handlingar 24 (1898) 1–39.
[41] Y.S. Ho, G. McKay, Sorption of dye from aqueous solution by peat, Chem. Eng. J. 70 (1998) 115–124.
[42] W.J. Weber, J.C. Morris, Jr., Kinetics of adsorption on carbon from solution, J. Sanitary Eng. Div. Am. Soc. Civ. Eng. 89 (1963) 31–60.
[43] V.J.P. Poots, G. McKay, J.J. Healy, The removal of acid dye from effluent using natural adsorbents: I. Peat, Water Res. 10 (1976) 1061–1066.
[44] W.H. Cheung, Y.S. Szeto, G. McKay, Intraparticle diffusion processes during acid dye adsorption onto chitosan, Bioresour. Technol. 98 (2007) 2897–2904.